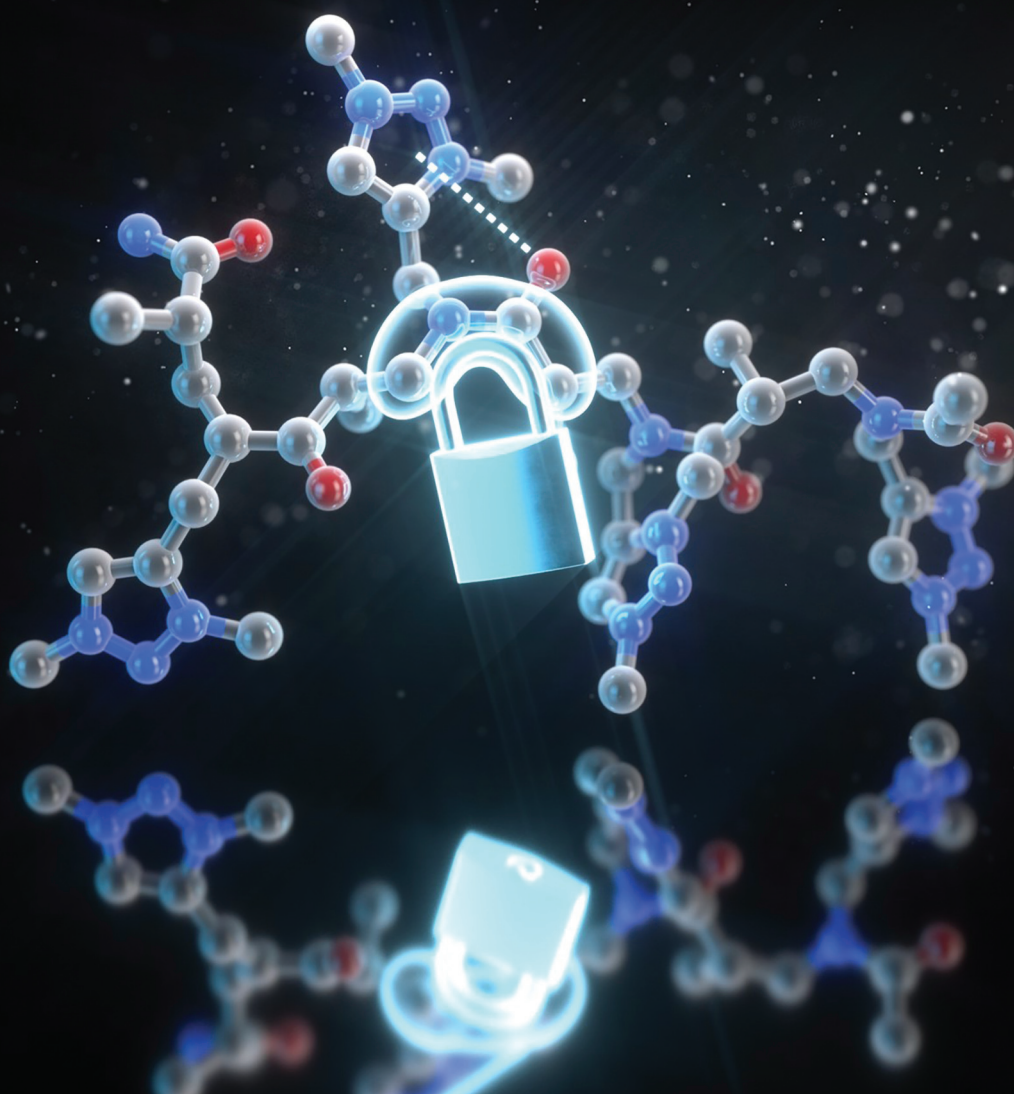


# Organic & Biomolecular Chemistry

rsc.li/obc

Volume 23  
Number 26  
14 July 2025  
Pages 6233-6458



ISSN 1477-0520

**PAPER**

Hyun-Suk Lim, Min Hyeon Shin *et al.*  
*cis*-Amide promotion in  $\alpha$ -ABpeptoid foldamers *via*  
triazolium side chains

## PAPER

View Article Online  
View Journal | View Issue



Cite this: *Org. Biomol. Chem.*, 2025, **23**, 6366

## *cis*-Amide promotion in $\alpha$ -ABpeptoid foldamers via triazolium side chains†

Jungyeon Kim, ‡<sup>a</sup> Ganesh A. Sable, ‡<sup>a</sup> Kang Ju Lee,<sup>a</sup> Hyun-Suk Lim \*<sup>a</sup> and Min Hyeon Shin \*<sup>b</sup>

Precise control of amide bond rotation is crucial for the construction of well-defined three-dimensional structures in peptidomimetic foldamers. We previously introduced  $\alpha$ -ABpeptoids as a new class of peptoid foldamers incorporating backbone chirality and demonstrated their folding propensities. However, the rotational isomerism of their backbone amide bonds remains largely unregulated. Here, we report the development of  $\alpha$ -ABpeptoids functionalized with triazolium side chains that promote *cis*-amide bond formation. A series of  $\alpha$ -ABpeptoid oligomers bearing neutral triazole or cationic triazolium side chains were synthesized and analyzed by NMR and circular dichroism spectroscopy. The triazolium-functionalized  $\alpha$ -ABpeptoids exhibited a strong preference for *cis*-amide geometry, resulting in enhanced conformational homogeneity. These findings establish triazolium substitution as an effective strategy for conformational control in  $\alpha$ -ABpeptoid foldamers, expanding their utility in the design of structured, functional peptidomimetics.

Received 27th February 2025,  
Accepted 21st April 2025

DOI: 10.1039/d5ob00355e

rsc.li/obc

## Introduction

Proteins derive their functions from their three-dimensional structures. To mimic protein functionality, researchers have sought to develop synthetic oligomers with predictable, well-defined conformations.<sup>1–3</sup> These molecules, termed foldamers by Gellman,<sup>4</sup> have emerged as a diverse class of synthetic architectures, enabling applications in molecular recognition, organocatalysis, and materials science.<sup>3,5–10</sup> Notably, foldamers offer significant advantages over native peptides, as they exhibit superior proteolytic stability and allow access to a vast chemical space by incorporating both proteinogenic and non-proteinogenic side chain building blocks. Over the years, a variety of synthetic foldamers have been developed, including  $\beta$ - and  $\gamma$ -peptides,<sup>11–14</sup> oligoureas,<sup>15,16</sup> oligotriazoles,<sup>17</sup>  $\gamma$ -AApeptides,<sup>18,19</sup> aromatic oligoamides,<sup>3,20</sup> and peptoids.<sup>21–26</sup>

Peptoids, oligomers of *N*-substituted glycine, are a class of peptidomimetic foldamers with advantages due to their synthetic accessibility, side-chain diversity,<sup>27</sup> resistance to proteo-

lytic degradation,<sup>28,29</sup> and enhanced cell permeability<sup>30–32</sup> compared to natural peptides (Fig. 1a). However, peptoids generally fail to adopt well-defined folding structures due to low rotational barrier of tertiary amide bonds and the absence of intramolecular hydrogen bonding, which is typically facilitated by amide protons in natural peptides. Therefore, developing strategies to control peptoid conformation, particularly amide bond geometry, has become a central focus in peptoid research.

A well-known strategy for controlling amide bond geometry in peptoids is the incorporation of  $\alpha$ -chiral side chains (Fig. 1a).<sup>33–35</sup> These  $\alpha$ -chiral side chains impart a handedness to the peptoid backbone, leading to the formation of polypro-

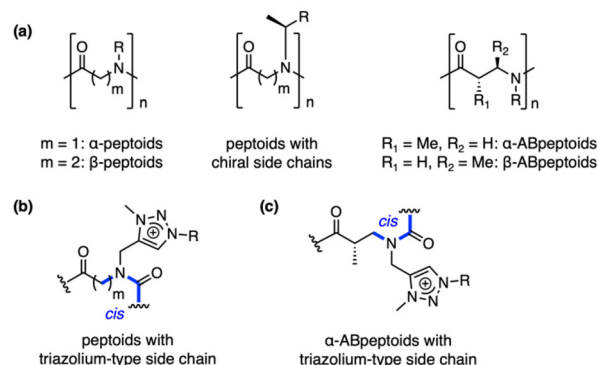


**Fig. 1** (a) General structures of  $\alpha$ - and  $\beta$ -peptoids, peptoids with chiral side chains,  $\alpha$ -ABpeptoids, and  $\beta$ -ABpeptoids. (b and c) Peptoids with triazolium-type side chain (b) and  $\alpha$ -ABpeptoid with triazolium-type side chain (c).

<sup>a</sup>Department of Chemistry and Division of Advanced Materials Science, Pohang University of Science and Technology (POSTECH), Pohang 37673, South Korea. E-mail: hslim@postech.ac.kr

<sup>b</sup>Department of Science Education, Daegu National University of Education, Daegu 42411, South Korea. E-mail: mhshin@dnue.ac.kr

†Electronic supplementary information (ESI) available: Characterization of organic compounds, analytical data, and NMR spectra. See DOI: <https://doi.org/10.1039/d5ob00355e>

‡These authors contributed equally.



line type-I (PPI) helical structure in peptoid oligomers. Beyond chirality, steric<sup>36–39</sup> and stereoelectronic<sup>40–43</sup> effects also play crucial roles in determining peptoid folding propensity. Steric hindrance from bulky side chains destabilizes the *trans* amide geometry due to steric repulsion between peptoid backbone and the bulky substituents in the *trans* configuration. Conversely, side chains with electron-deficient moieties such as pyridinium and triazolium (Fig. 1b) could promote *cis*-amide geometry *via* a stereoelectronic  $n \rightarrow \pi^*$  interaction.<sup>44</sup> Some side chains leverage both steric and stereoelectronic effects to precisely regulate peptoid amide bond geometry.<sup>45–47</sup> These side chains strongly bias peptoids toward *cis*-amide geometry at the monomer level, thereby enhancing their conformational homogeneity and structural predictability.

Inspired by the strategy of incorporating  $\alpha$ -chiral side chains into peptoids, we developed  $\alpha$ - and  $\beta$ -ABpeptoids as a novel class of peptidomimetic foldamers (Fig. 1a).<sup>48–52</sup> These structures feature a  $\beta$ -peptoid backbone with a chiral methyl group positioned at either  $\alpha$ - or  $\beta$ -carbon, which we hypothesized would enhance the folding propensity of the oligomers, similar to the effect of  $\alpha$ -chiral side chains in  $\alpha$ -peptoids. Consistent with this expectation, circular dichroism (CD) studies confirmed that  $\alpha$ - and  $\beta$ -ABpeptoids adopt folded structures in solution. However, NMR studies revealed that  $\alpha$ - and  $\beta$ -ABpeptoids exist as mixtures of *cis* and *trans* amide isomers, indicating that amide bond geometry remains uncontrolled in these systems.

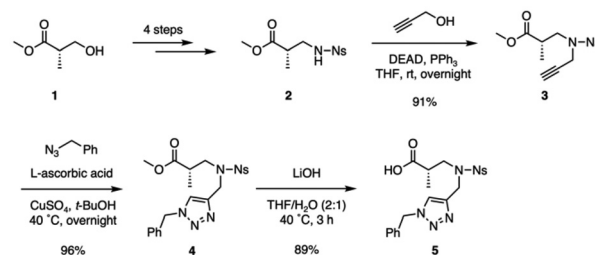
As observed in the case of peptoids, we anticipate that precise control of amide bond rotation would be crucial for achieving stable and well-defined three-dimensional structures in  $\alpha$ -ABpeptoids. Recently, Taillefumier and colleagues demonstrated that triazolium-containing side chains exhibit a remarkable *cis*-directing effect in both monomer model studies and peptoid oligomers (Fig. 1b).<sup>42,43</sup> The triazolium side chain stabilizes *cis*-amide geometry through a strong  $n \rightarrow \pi^*_{Ar}$  interaction, where the amide carbonyl of the neighboring residue donates electron density to the electron-deficient triazolium group. Inspired by Taillefumier's findings, we hypothesized that triazolium-functionalized side chains would effectively restrict amide bond rotation in  $\alpha$ -ABpeptoids, thereby promoting the formation of a stable, homogeneous three-dimensional structure without compromising chemical diversity (Fig. 1c). Here, we report the design, solid-phase synthesis of a series of  $\alpha$ -ABpeptoid oligomers containing triazole and triazolium side chains, along with their structural characterization using NMR and CD spectroscopy.

## Results and discussion

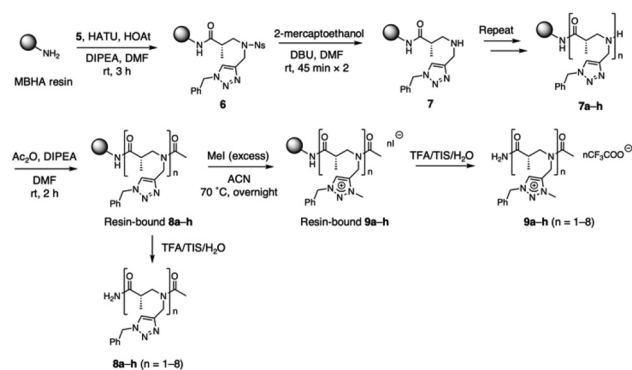
To investigate whether the introduction of triazolium side chains promotes the folding of  $\alpha$ -ABpeptoids by stabilizing the *cis*-amide conformation, we synthesized a series of  $\alpha$ -ABpeptoid oligomers with triazolium side chains using solid phase synthesis. For comparison,  $\alpha$ -ABpeptoids with triazole side chains were prepared. Initially, we synthesized a nosyl-

protected  $\alpha$ -ABpeptoid monomer 5 which carries a benzyl-substituted triazole, following Scheme 1. First, compound 2 was synthesized from the commercially available compound 1 as according to our previous report.<sup>48</sup> Then, *N*-propargylation of compound 2 was carried out *via* Fukuyama–Mitsunobu reaction, yielding compound 3 in 91% yield. Next, compound 3 underwent copper-catalyzed azide–alkyne cycloaddition (CuAAC) with benzyl azide, affording compound 4 in 96% yield. Importantly,  $\alpha$ -ABpeptoid monomers with various functional groups can be prepared by replacing benzyl azide with other azides in this step, enabling further chemical diversity. Finally, the ethyl ester of compound 4 was hydrolyzed using lithium hydroxide (LiOH) to give the  $\alpha$ -ABpeptoid monomer 5 in 89% yield. This synthetic route is straightforward, high-yielding, and cost-effective, utilizing readily available and inexpensive starting materials.

For the solid-phase synthesis of  $\alpha$ -ABpeptoids oligomers containing triazole and triazolium side chains, monomer 5 was loaded on Rink amide MBHA resin *via* coupling reaction using hexafluorophosphate azabenzotriazole tetramethyl uranium (HATU)/1-hydroxy-7-azabenzotriazole (HOAt)/*N,N*-diisopropylethylamine (DIPEA) in DMF (Scheme 2). Next, the nosyl protecting group of resin-bound 6 was removed using 2-mercaptoethanol and 1,8-diazabicycloundec-7-ene (DBU) in DMF, yielding the resin-bound secondary amine 7. This coupling reaction-and-deprotection sequence was then repeated to



**Scheme 1** Synthesis of a  $\alpha$ -ABpeptoid monomer with *N*-triazole side chain (5).



**Scheme 2** Solid-phase synthesis of  $\alpha$ -ABpeptoid oligomers containing triazole or triazolium side chains.



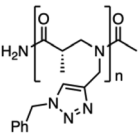
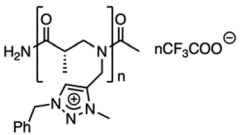
obtain oligomers ranging from monomer to octamer (**7a–h**). The N-termini of the oligomers were acetylated using acetic anhydride (Ac<sub>2</sub>O) and DIPEA in DMF, resulting in acetylated  $\alpha$ -ABpeptoids (**8a–h**). Finally, the triazole groups of **8a–h** were quaternized by treatment of excess methyl iodide (MeI) at 70 °C overnight, affording  $\alpha$ -ABpeptoid oligomers with triazolium side chains (**9a–h**). The  $\alpha$ -ABpeptoid oligomers **8a–h** and **9a–h** were then cleaved from the resin by treating with the cleavage cocktail trifluoroacetic acid (TFA)/triisopropylsilane (TIS)/H<sub>2</sub>O (95 : 2.5 : 2.5). The resulting  $\alpha$ -ABpeptoid oligomers, functionalized with triazole and triazolium side chains, were then purified by reverse-phase HPLC and characterized by mass spectrometry (Table 1 and Fig. S1†). As the oligomers were treated with a TFA solution during cleavage from resin, all iodide counterions (I<sup>−</sup>) of the quaternary salts were exchanged for trifluoroacetate ions (CF<sub>3</sub>COO<sup>−</sup>). Notably, the  $\alpha$ -ABpeptoids displayed excellent crude purity, as exemplified by the longest oligomers **8h** and **9h**, which showed crude purities of 86% and 93%, respectively (Fig. S2 and Table S1†). This result underscores the robustness of the synthetic method.

To investigate the impact of the triazolium side chain on the amide bond geometry of  $\alpha$ -ABpeptoids, we performed conformational analysis of  $\alpha$ -ABpeptoid monomer models using NMR spectroscopy. <sup>1</sup>H NMR spectra of  $\alpha$ -ABpeptoid monomers carrying a triazole side chain (**8a**) and a triazolium side chain (**9a**) were recorded in CD<sub>3</sub>CN, CDCl<sub>3</sub>, and CD<sub>3</sub>OD (Fig. S3 and S5†). The <sup>1</sup>H NMR spectra of both **8a** and **9a** displayed two

sets of peaks, corresponding to *cis* and *trans* amide rotamers. The assignment of *cis* and *trans* isomers was performed using homonuclear correlation spectroscopy (COSY) and nuclear Overhauser effect spectroscopy (NOESY) (Fig. S4 and S6†). The *cis/trans* equilibrium constants (*K*<sub>*cis/trans*</sub>) were determined from the integration of acetyl protons of *cis* and *trans* isomers on <sup>1</sup>H NMR spectra (Table 2). For **8a** bearing a triazole side chain, *cis* and *trans* isomers were present in nearly equal proportions in CD<sub>3</sub>CN and CD<sub>3</sub>OD with *K*<sub>*cis/trans*</sub> values of 1.40 and 1.65, respectively. In contrast, **9a**, which carries a triazolium side chain, exhibited a strong preference for the *cis* amide isomer with the *cis*-amide population exceeding 90% in all tested solvents. This demonstrates that the triazolium side chain strongly directs the amide bond of  $\alpha$ -ABpeptoids toward *cis* geometry at the monomer level. Additionally, **9a** showed a higher *K*<sub>*cis/trans*</sub> value in CDCl<sub>3</sub> compared to CD<sub>3</sub>CN and CD<sub>3</sub>OD, indicating an enhanced *cis*-amide preference in non-polar solvents. The significant difference in *K*<sub>*cis/trans*</sub> values between **8a** and **9a**, along with the increased *cis*-inducing effect of the triazolium side chain in the non-polar solvent, suggests the presence of a stereoelectronic effect, such as  $n \rightarrow \pi^*$  interaction between the carbonyl group of the acetamide and the electron-deficient triazolium ring.

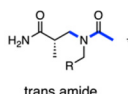
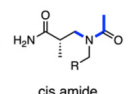
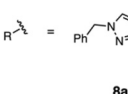
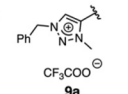
The C–H group of the triazolium group is capable of interacting with electronegative groups. For example, triazolium can recognize anions by acting as a hydrogen bond donor.<sup>53</sup> Moreover, triazolium C–H in  $\alpha$ -peptoid forms an intra-residue hydrogen bond with carbonyl group.<sup>42</sup> To determine whether a similar triazolium C–H interaction is present in  $\alpha$ -ABpeptoids, we compared the chemical shift of triazolium C–H in **9a** in CDCl<sub>3</sub> (a non-polar solvent) with those in CD<sub>3</sub>CN and CD<sub>3</sub>OD (polar solvents), as intramolecular hydrogen bonds are often disrupted in polar environments. The chemical shifts of triazolium C–H in **9a** were 8.97 ppm in CDCl<sub>3</sub>, 8.35 ppm in CD<sub>3</sub>CN, and 8.65 ppm in CD<sub>3</sub>OD (Fig. S5†). The small difference in chemical shift between polar and non-polar solvents implies that no significant intramolecular hydrogen bond involving triazolium C–H is present in  $\alpha$ -ABpeptoids. This observation contrasts with the substantial downfield shift of the triazolium C–H in  $\alpha$ -peptoids in CDCl<sub>3</sub>, compared to that in CD<sub>3</sub>CN ( $\Delta\delta$  = 1.61 ppm). We speculate that, unlike  $\alpha$ -peptoid backbone,

**Table 1** Sequence, purity, and mass confirmation of synthesized  $\alpha$ -ABpeptoids

<div style="display: flex; justify-content: space-around; align-items: center;"> <div style="text-align: center;">  <p><b>8a–h</b> (n = 1–8)</p> </div> <div style="text-align: center;">  <p><b>9a–h</b> (n = 1–8)</p> </div> </div>				
Compound	Chain length	% purity <sup>a</sup>	Calcd mass <sup>b</sup>	Obsd mass <sup>c</sup>
<b>8a</b>	1	96	316.1773	316.1773
<b>8b</b>	2	96	572.3098	572.3096
<b>8c</b>	3	98	828.4422	828.4419
<b>8d</b>	4	98	1084.5746	1084.5747
<b>8e</b>	5	99	1340.7070	1340.7067
<b>8f</b>	6	97	1596.8394	1596.8394
<b>8g</b>	7	96	1852.9718	1852.9706
<b>8h</b>	8	98	2109.1042	2109.1052
<b>9a</b>	1	96	330.1930	330.1932
<b>9b</b>	2	99	714.3339	714.3337
<b>9c</b>	3	97	1098.4749	1098.4745
<b>9d</b>	4	99	1482.6152	1482.6160
<b>9e</b>	5	99	1866.7567	1866.7566
<b>9f</b>	6	99	2250.8976	2250.8965
<b>9g</b>	7	97	2635.0386	2635.0339
<b>9h</b>	8	97	3019.1795	3019.1868

<sup>a</sup> Purity was determined by analytical HPLC chromatogram of purified products. <sup>b</sup> Calculated mass for [M + H]<sup>+</sup> (**8a–h**) or [M – CF<sub>3</sub>COO]<sup>+</sup> (**9a–h**) are shown. <sup>c</sup> High resolution mass spectra (HRMS) were acquired using Electrospray ionization (ESI) techniques.

**Table 2** *cis/trans* ratios (*K*<sub>*cis/trans*</sub>) or relative proportion of *cis* isomer in three different solvents for  $\alpha$ -ABpeptoid monomers with triazole side chain (**8a**) and triazolium side chain (**9a**)<sup>a</sup>

<div style="display: flex; justify-content: space-around; align-items: center;"> <div style="text-align: center;">  <p>trans amide</p> </div> <div style="text-align: center;">  <p>cis amide</p> </div> <div style="text-align: center;"> <p><math>K_{cis/trans}</math></p> </div> </div>			
<div style="display: flex; justify-content: space-around; align-items: center;"> <div style="text-align: center;">  <p><b>8a</b></p> </div> <div style="text-align: center;">  <p><b>9a</b></p> </div> </div>			
Compound	CD <sub>3</sub> CN (% <i>cis</i> )	CDCl <sub>3</sub> (% <i>cis</i> )	CD <sub>3</sub> OD (% <i>cis</i> )
<b>8a</b>	1.40 (58)	3.54 (78)	1.65 (62)
<b>9a</b>	10.14 (91)	18.43 (95)	10.07 (91)

<sup>a</sup> *K*<sub>*cis/trans*</sub> values were determined based on the integration of <sup>1</sup>H NMR signals of acetyl protons.



which adopts a conformation favorable for intra-residue hydrogen bonding, the elongated  $\alpha$ -ABpeptoid backbone may prevent the triazolium and the carbonyl group from coming into close proximity, thereby disrupting the potential hydrogen bonding interaction.

Next, we investigated the amide rotameric preference of dimers **8b** and **9b**. The  $^1\text{H}$  NMR spectra of both compounds in  $\text{CD}_3\text{CN}$ ,  $\text{CDCl}_3$ , and  $\text{CD}_3\text{OD}$  exhibited four distinct isomers, corresponding to the *cis-cis*, *cis-trans*, *trans-cis*, and *trans-trans* amide geometries. For **8b**, the  $^1\text{H}$  NMR spectra in  $\text{CD}_3\text{CN}$  and  $\text{CD}_3\text{OD}$  showed all four isomers present in nearly equal proportions, while in  $\text{CDCl}_3$ , two major isomers accounted for more than 70% of the total population (Fig. 2a and Fig. S7†). In contrast, the  $^1\text{H}$  NMR spectra of **9b** revealed a single predominant amide bond rotamer in all tested solvents (Fig. 2b and Fig. S8†), indicating a strong *cis*-directing effect of the triazolium side chain. To determine the conformation of the major rotamer of **9b**, we carefully assigned peaks in its  $^1\text{H}$  NMR spectrum in  $\text{CD}_3\text{CN}$  (Fig. 3). Detailed analysis of the COSY,  $^1\text{H}$ - $^{13}\text{C}$  heteronuclear multiple bond correlation (HMBC), and NOESY spectra enabled us to successfully distinguish the backbone protons as well as the triazolium C-H protons of the two residues (Fig. S9†). Further analysis of the NOESY spectrum allowed us to determine the amide bond geometry of **9b** (Fig. 3 and Fig. S9†). Specifically, NOE correlations between the backbone  $\alpha$ - and  $\beta$ -protons of the C-terminal residue (residue 2) and the backbone  $\alpha$ -proton of the N-terminal residue (residue 1) support a *cis* geometry for the amide bond connecting these two residues. Additionally, NOEs involving the acetyl protons indicate that the acetamide adopts a *cis* conformation. Collectively, these observations demonstrate that the major rotamer of **9b** adopts a *cis-cis* amide geometry, suggesting that the triazolium side chain strongly biases the  $\alpha$ -ABpeptoid dimer **9b** toward a locally defined conformation in solution through its *cis*-stabilizing effect.

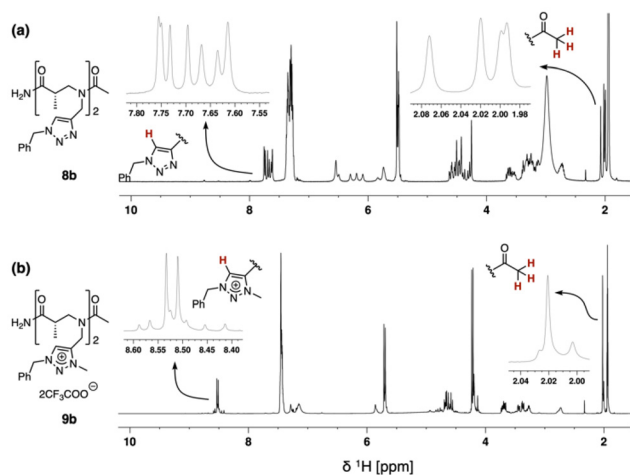


Fig. 2  $^1\text{H}$  NMR spectra of  $\alpha$ -ABpeptoid dimers with (a) triazole side chains (**8b**) and (b) triazolium side chains (**9b**) in  $\text{CD}_3\text{CN}$ .

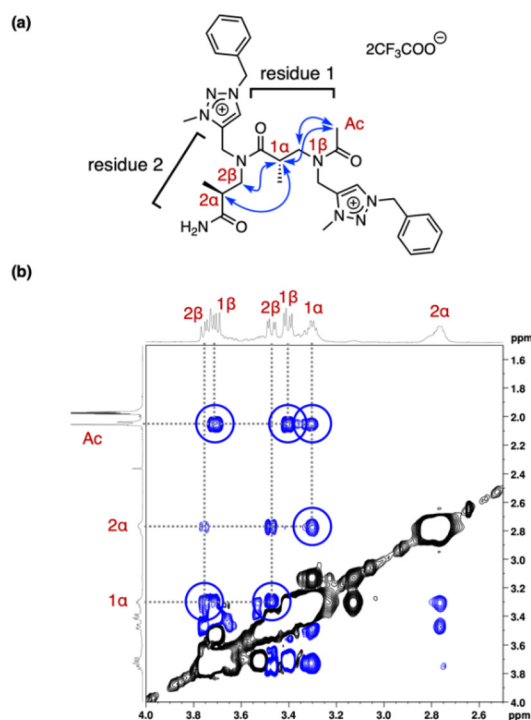
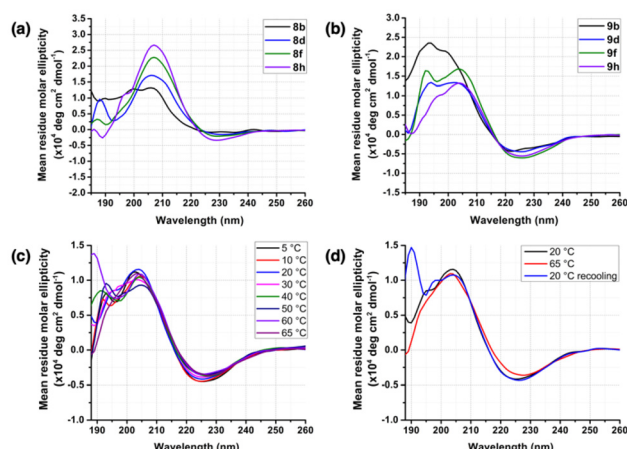


Fig. 3 Structural analysis of  $\alpha$ -ABpeptoid dimer carrying triazolium side chains (**9b**). (a) NOEs of **9b** observed in  $\text{CD}_3\text{CN}$ . NOEs indicating the *cis* amide configuration in the major isomer are shown in blue arrows. (b) Close-up view of the 2D NOESY spectrum of **9b** in  $\text{CD}_3\text{CN}$ , where cross-peaks indicating *cis* amide geometry are marked with blue circles.

To assess whether the *cis*-directing effect of the triazolium side chain enhances the conformational homogeneity of  $\alpha$ -ABpeptoid oligomers, we recorded  $^1\text{H}$  NMR spectra of **8c-h** and **9c-h** (Fig. S10 and S11†). Due to severe signal overlap in  $^1\text{H}$  NMR spectra, assignment of the NMR spectra was challenging. However, triazole/triazolium C-H peaks allowed us to evaluate conformational homogeneity of the  $\alpha$ -ABpeptoids. The  $^1\text{H}$  NMR spectra of  $\alpha$ -ABpeptoids with triazole side chains (**8c-h**) displayed a greater number of triazole C-H peaks than expected based on the numbers of triazole groups, indicating the presence of multiple amide bond rotamers. In contrast, for  $\alpha$ -ABpeptoids with triazolium side chains (**9c-h**), a single major rotamer was observed in the  $^1\text{H}$  NMR spectra up to 5mer (**9e**). This result suggests that the triazolium side chains significantly enhance the amide rotameric preference of  $\alpha$ -ABpeptoids, promoting a well-defined conformation in solution.

To evaluate the folding propensity and gain structural insights into  $\alpha$ -ABpeptoids carrying triazole (**8b-h**) and triazolium side chains (**9b-h**), we obtained their CD spectra in trifluoroethanol (TFE). The CD spectral profiles of  $\alpha$ -ABpeptoids varied depending on the chain length (Fig. 4a and b). The CD spectra of **8b-h** exhibited a maximum at 207 nm and a minimum at 228 nm, with increasing signal intensity as the chain length increased. Similarly,  $\alpha$ -ABpeptoids with triazolium side chains (**9b-h**) displayed CD spectral resembling





**Fig. 4** (a and b) CD spectra of **8b**, **8d**, **8f**, and **8h** (a) and **9b**, **9d**, **9f**, and **9h** (b) in TFE at 20 °C. (c) Temperature dependence of the CD spectrum of **9h** in TFE. (d) CD spectra of **9h** after recooling. All spectra were recorded at a concentration of 60  $\mu\text{M}$ .

those of **8b–h**, but with an overall blue-shift. For example, the CD spectrum of 8-mer  $\alpha$ -ABpeptoid **9h** exhibited a maximum at 204 nm and a minimum at 224 nm. A notable difference between the CD spectra of **8b–h** and **9b–h** was that the CD signals of **9b–h** reached saturation at shorter oligomer lengths. Specifically, the maximum around 204 nm and the minimum around 224 nm were saturated at 4-mer (**9d**) and 6-mer (**9f**), respectively. This finding suggests that  $\alpha$ -ABpeptoids with triazolium side chains (**9b–h**) may exhibit stronger folding propensities than their triazole-containing counterparts (**8b–h**), likely due to the *cis*-directing effect of the triazolium moiety.

Next, we sought to evaluate the thermal stability of the conformation adopted by **9h**. To this end, we recorded CD spectra of **9h** in TFE at temperatures ranging from 5 to 65 °C. While the overall spectral shape remained unchanged, the intensity of the minimum at 224 nm gradually decreased in a temperature-dependent manner (Fig. 4c). This change was reversible, as the spectrum recovered both its shape and intensity upon recooling (Fig. 4d), indicating that **9h** undergoes a temperature-dependent reversible folding process. Based on the CD intensity change at 224 nm, the melting temperature ( $T_m$ ) of **9h** was estimated to be 30 °C (Fig. S12†). We also investigated the temperature dependence of the CD spectrum of **8h** (Fig. S13†). Although **8h** exhibited temperature-dependent spectral changes, its transition followed a primarily linear trend rather than a sigmoidal transition, making it difficult to accurately determine its melting temperature. This difference suggests that **9h** adopts a thermodynamically more stable folded structure compared to **8h**, presumably due to the *cis*-stabilizing effect of the triazolium side chains.

## Conclusions

In summary, we have described the synthesis and conformational evaluation of  $\alpha$ -ABpeptoids functionalized with tri-

azole and triazolium side chains. We established robust synthetic methods, including the efficient synthesis of the  $\alpha$ -ABpeptoid monomers carrying triazole side chains, solid-phase synthesis of  $\alpha$ -ABpeptoid oligomers, and on-resin triazole quaternization for triazolium formation. Using these methods, we successfully prepared  $\alpha$ -ABpeptoids with triazole/triazolium side chains ranging from monomers to octamers in high yields. NMR studies demonstrated that the triazolium side chain exert a strong *cis*-directing effect on the amide geometry in  $\alpha$ -ABpeptoid monomers and dimers. Additionally, NMR analysis of longer  $\alpha$ -ABpeptoids revealed that triazolium substitution enhances rotameric homogeneity at amide bonds, promoting a more defined structural arrangement. Further insights were obtained from CD spectroscopy, which indicated chain length- and temperature-dependent spectral changes, suggesting that the formation of an ordered structure in triazolium-functionalized  $\alpha$ -ABpeptoids. Collectively, our findings suggest that fixing the amide geometry on the *cis* conformation *via* triazolium side chain significantly improves the ability of  $\alpha$ -ABpeptoids to adopt a well-defined conformation. Beyond its role in *cis*-amide stabilization, the triazolium side chain provides synthetic versatility, as the azide building blocks used in the click chemistry can be readily modified, enabling access to diverse chemical structures. Given their strong folding propensity and synthetic versatility, and the inherent advantages of peptoid-like structures, including enhanced cell permeability and proteolytic stability,  $\alpha$ -ABpeptoids with *cis*-directing triazolium side chains represent a novel class of peptoid foldamers with promising applications in biomedical research and materials science. Although the precise conformation of the  $\alpha$ -ABpeptoids studied here remains unresolved, future structural investigations, such as advanced NMR spectroscopy and X-ray crystallographic analysis, are expected to offer deeper insights into their overall architectures, particularly with respect to their secondary structures and handedness.

## Author contributions

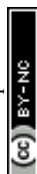
J. K.: formal analysis, investigation, validation, visualization, and writing – original draft; G. A. S.: conceptualization, formal analysis, investigation, visualization, and writing – original draft; K. J. L.: conceptualization; H.-S. L. and M. H. S.: project administration, supervision, writing – review & editing, and funding acquisition. J. K. and G. A. S. contributed equally.

## Data availability

The data supporting this article have been included as part of the ESI.†

## Conflicts of interest

There are no conflicts to declare.

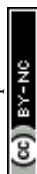


## Acknowledgements

This work was supported by the National Research Foundation of Korea (Grants NRF-2022R1A2C2008460, NRF-2022M3A9G8084563, NRF-2022M3A9G8017710, NRF-RS-2023-00260005, NRF-RS-2024-00411069, RS-2023-00249191, and RS-2023-00274113).

## References

- D. J. Hill, M. J. Mio, R. B. Prince, T. S. Hughes and J. S. Moore, *Chem. Rev.*, 2001, **101**, 3893–4012.
- T. A. Martinek and F. Fulop, *Chem. Soc. Rev.*, 2012, **41**, 687–702.
- D.-W. Zhang, X. Zhao, J.-L. Hou and Z.-T. Li, *Chem. Rev.*, 2012, **112**, 5271–5316.
- S. H. Gellman, *Acc. Chem. Res.*, 1998, **31**, 173–180.
- C. M. Goodman, S. Choi, S. Shandler and W. F. DeGrado, *Nat. Chem. Biol.*, 2007, **3**, 252–262.
- P. Sang and J. Cai, *Chem. Soc. Rev.*, 2023, **52**, 4843–4877.
- W. S. Horne, *Expert Opin. Drug Discovery*, 2011, **6**, 1247–1262.
- Z. C. Girvin and S. H. Gellman, *J. Am. Chem. Soc.*, 2020, **142**, 17211–17223.
- E. J. Robertson, A. Battigelli, C. Proulx, R. V. Mannige, T. K. Haxton, L. Yun, S. Whitelam and R. N. Zuckermann, *Acc. Chem. Res.*, 2016, **49**, 379–389.
- Z. Li, B. Cai, W. Yang and C.-L. Chen, *Chem. Rev.*, 2021, **121**, 14031–14087.
- R. P. Cheng, S. H. Gellman and W. F. DeGrado, *Chem. Rev.*, 2001, **101**, 3219–3232.
- S. Kwon, B. J. Kim, H.-K. Lim, K. Kang, S. H. Yoo, J. Gong, E. Yoon, J. Lee, I. S. Choi, H. Kim and H.-S. Lee, *Nat. Commun.*, 2015, **6**, 8747.
- S. Shin, M. Lee, I. A. Guzei, Y. K. Kang and S. H. Choi, *J. Am. Chem. Soc.*, 2016, **138**, 13390–13395.
- B. Legrand and L. T. Maillard, *ChemPlusChem*, 2021, **86**, 629–645.
- A. Violette, M. C. Averlant-Petit, V. Semetey, C. Hemmerlin, R. Casimir, R. Graff, M. Marraud, J.-P. Briand, D. Rognan and G. Guichard, *J. Am. Chem. Soc.*, 2005, **127**, 2156–2164.
- G. W. Collie, K. Pulka-Ziach, C. M. Lombardo, J. Fremaux, F. Rosu, M. Decossas, L. Mauran, O. Lambert, V. Gabelica, C. D. Mackereth and G. Guichard, *Nat. Chem.*, 2015, **7**, 871–878.
- N. G. Angelo and P. S. Arora, *J. Am. Chem. Soc.*, 2005, **127**, 17134–17135.
- Y. Shi, P. Teng, P. Sang, F. She, L. Wei and J. Cai, *Acc. Chem. Res.*, 2016, **49**, 428–441.
- P. Sang, Y. Shi, L. Wei and J. Cai, *RSC Chem. Biol.*, 2022, **3**, 805–814.
- Y. Ferrand and I. Huc, *Acc. Chem. Res.*, 2018, **51**, 970–977.
- R. J. Simon, R. S. Kania, R. N. Zuckermann, V. D. Huebner, D. A. Jewell, S. Banville, S. Ng, L. Wang, S. Rosenberg and C. K. Marlowe, *Proc. Natl. Acad. Sci. U. S. A.*, 1992, **89**, 9367–9371.
- B. Yoo and K. Kirshenbaum, *Curr. Opin. Chem. Biol.*, 2008, **12**, 714–721.
- R. Zuckermann and T. Kodadek, *Curr. Opin. Mol. Ther.*, 2009, **11**, 299–307.
- M. Oh, J. H. Lee, H. Moon, Y.-J. Hyun and H.-S. Lim, *Angew. Chem., Int. Ed.*, 2016, **55**, 602–606.
- M. H. Shin, K. J. Lee and H.-S. Lim, *Bioconjugate Chem.*, 2019, **30**, 2931–2938.
- K. J. Lee, G. Bang, Y. W. Kim, M. H. Shin and H.-S. Lim, *Bioorg. Med. Chem.*, 2021, **48**, 116423.
- R. N. Zuckermann, J. M. Kerr, S. B. H. Kent and W. H. Moos, *J. Am. Chem. Soc.*, 1992, **114**, 10646–10647.
- S. M. Miller, R. J. Simon, S. Ng, R. N. Zuckermann, J. M. Kerr and W. H. Moos, *Drug Dev. Res.*, 1995, **35**, 20–32.
- Y. Wang, H. Lin, R. Tullman, C. F. Jewell Jr., M. L. Weetall and F. L. Tse, *Biopharm. Drug Dispos.*, 1999, **20**, 69–75.
- P. Yu, B. Liu and T. Kodadek, *Nat. Biotechnol.*, 2005, **23**, 746–751.
- Y.-U. Kwon and T. Kodadek, *J. Am. Chem. Soc.*, 2007, **129**, 1508–1509.
- M.-K. Shin, Y.-J. Hyun, J. H. Lee and H.-S. Lim, *ACS Comb. Sci.*, 2018, **20**, 237–242.
- K. Kirshenbaum, A. E. Barron, R. A. Goldsmith, P. Armand, E. K. Bradley, K. T. V. Truong, K. A. Dill, F. E. Cohen and R. N. Zuckermann, *Proc. Natl. Acad. Sci. U. S. A.*, 1998, **95**, 4303–4308.
- P. Armand, K. Kirshenbaum, R. A. Goldsmith, S. Farr-Jones, A. E. Barron, K. T. V. Truong, K. A. Dill, D. F. Mierke, F. E. Cohen, R. N. Zuckermann and E. K. Bradley, *Proc. Natl. Acad. Sci. U. S. A.*, 1998, **95**, 4309–4314.
- C. W. Wu, T. J. Sanborn, K. Huang, R. N. Zuckermann and A. E. Barron, *J. Am. Chem. Soc.*, 2001, **123**, 6778–6784.
- O. Roy, C. Caumes, Y. Esvan, C. Didierjean, S. Faure and C. Taillefumier, *Org. Lett.*, 2013, **15**, 2246–2249.
- O. Roy, G. Dumonteil, S. Faure, L. Jouffret, A. Kriznik and C. Taillefumier, *J. Am. Chem. Soc.*, 2017, **139**, 13533–13540.
- J. Morimoto, Y. Fukuda, D. Kuroda, T. Watanabe, F. Yoshida, M. Asada, T. Nakamura, A. Senoo, S. Nagatoishi, K. Tsumoto and S. Sando, *J. Am. Chem. Soc.*, 2019, **141**, 14612–14623.
- J. Morimoto, J. Kim, D. Kuroda, S. Nagatoishi, K. Tsumoto and S. Sando, *J. Am. Chem. Soc.*, 2020, **142**, 2277–2284.
- N. H. Shah, G. L. Butterfoss, K. Nguyen, B. Yoo, R. Bonneau, D. L. Rabenstein and K. Kirshenbaum, *J. Am. Chem. Soc.*, 2008, **130**, 16622–16632.
- B. C. Gorske, B. L. Bastian, G. D. Geske and H. E. Blackwell, *J. Am. Chem. Soc.*, 2007, **129**, 8928–8929.
- C. Caumes, O. Roy, S. Faure and C. Taillefumier, *J. Am. Chem. Soc.*, 2012, **134**, 9553–9556.
- H. Aliouat, C. Caumes, O. Roy, M. Zouikri, C. Taillefumier and S. Faure, *J. Org. Chem.*, 2017, **82**, 2386–2398.
- R. W. Newberry and R. T. Raines, *Acc. Chem. Res.*, 2017, **50**, 1838–1846.
- J. R. Stringer, J. A. Crapster, I. A. Guzei and H. E. Blackwell, *J. Am. Chem. Soc.*, 2011, **133**, 15559–15567.



- 46 J. S. Laursen, P. Harris, P. Fristrup and C. A. Olsen, *Nat. Commun.*, 2015, **6**, 7013.
- 47 J. Oh, Y. Lee, G. Noh, D. Park, H. Lee, J. Lee, C. Kim and J. Seo, *Small Struct.*, 2024, **5**, 2300396.
- 48 K. J. Lee, W. S. Lee, H. Yun, Y.-J. Hyun, C. D. Seo, C. W. Lee and H.-S. Lim, *Org. Lett.*, 2016, **18**, 3678–3681.
- 49 G. A. Sable, K. J. Lee, M.-K. Shin and H.-S. Lim, *Org. Lett.*, 2018, **20**, 2526–2529.
- 50 G. A. Sable, K. J. Lee and H.-S. Lim, *Molecules*, 2019, **24**, 178.
- 51 K. J. Lee, G. A. Sable, M.-K. Shin and H.-S. Lim, *Biopolymers*, 2019, **110**, e23289.
- 52 S. Lee, H. Kwon, E.-K. Jee, J. Kim, K. J. Lee, J. Kim, N. Ko, E. Lee and H.-S. Lim, *Org. Lett.*, 2024, **26**, 1100–1104.
- 53 J. Cai and J. L. Sessler, *Chem. Soc. Rev.*, 2014, **43**, 6198–6213.

